Performance Degradation of a Model Helicopter Rotor with a Generic Ice Shape

K. D. Korkan,* E. J. Cross Jr.,† and T L. Miller‡
Texas A&M University, College Station, Texas

An experimental program using a commercially available remotely controlled model helicopter in the Texas A&M University (TAMU) subsonic wind tunnel has been conducted to investigate the performance degradation resulting from the simulated formation of ice on the leading edge of the main rotor blades in both hover and forward flight. The rotor blades utilized a NACA 0012 airfoil with a 2.5-in. constant chord. A generic ice shape derived from a predetermined natural ice condition was applied to the 53.375-in.-diam main rotor, and thrust and torque coefficients were measured for the main rotor as functions of velocity, main rotor rpm, fuselage angle of incidence, collective pitch angle, and spanwise extent of icing. The model helicopter test exhibited significant performance degradation of the main rotor when generic ice was added. An increase of approximately 150% in torque coefficient to maintain a constant thrust coefficient was noted when generic ice had been applied to the 85% rotor radial location. Also, considerable additional degradation occurred when generic ice was applied to the 100% rotor radial location as compared with the 85% simulated ice performance values, indicating the sensitivity of the rotor tip region.

Nomenclature

A	= rotor disk area = ΠR_{tip}^2
B	= number of blades
c	= airfoil chord
C_d	= drag coefficient = $D/q_\infty c$
C_l	= lift coefficient = $L/q_\infty c$
C_P	= power coefficient = $p/\rho A V_{tip}^3$
C_Q	= torque coefficient = $Q/\rho A V_{tip}^2 R_{tip}$
C_T	= thrust coefficient = $T/\rho A V_{tip}^2$
D	= drag force
k	= roughness particle diameter
L	= lift force
P	= rotor shaft power
q	= dynamic pressure = $\rho V_\infty^2/2$
Q	= torque moment
r	= local radius
R, R_{tip}	= rotor radius
Re_{tip}	= rotor tip Reynolds number = $\rho V_{tip} c/\mu_\infty$
Re_∞	= freestream Reynolds number = $\rho V_{tip} c/\mu_\infty$
T	= thrust force
V_{tip}	= rotor tip velocity = ΩR_{tip}
V_∞	= freestream velocity
α	= rotor disk angle with respect to freestream
θ	= rotor collective pitch
μ	= helicopter advance ratio = $V_\infty \cos\alpha / V_{tip}$
μ_∞	= air viscosity
ρ	= air density
σ	= rotor solidity = $Bc/\Pi R_{tip}$
Ω	= rotational velocity

Introduction

WHEN ice is allowed to accumulate on an airfoil surface, the effective geometry of the airfoil is altered, and its aerodynamic characteristics can be severely effected. For rotating systems such as propeller and helicopter rotor blades, this effect translates into significant reductions in performance with respect to the thrust and power required when ice is allowed to accrete on the leading edge of the blades. Analytical models currently exist that predict theoretical values for performance of propellers[1] and helicopter rotor blades under the influence of rime ice both in hover[2] and in forward flight.[3] However, test data are needed to expand the very limited experimental data base, which can then be used to verify and improve the present analytical models.

The test program contained in this paper initially involved testing of a 21-in. chord NACA 0012 airfoil section both in the clean and generic ice configurations. Reynolds number effects on the performance of the airfoil were investigated for both configurations. A detailed discussion of the results of this airfoil test has been documented by Korkan et al.,[4] with the conclusion that there is a slight Reynolds number effect on the aerodynamic performance of the airfoil with the generic ice throughout the range of values tested, i.e., from 0.7×10^6 to 3×10^6 based on airfoil chord. Also, substantial aerodynamic degradation of the airfoil with simulated ice was noted.

A radio-controlled model helicopter has also been tested in the 7 ft × 10-ft subsonic wind tunnel at Texas A&M University in a test program that has been documented by Korkan et al.[5] Extensive testing of the helicopter was performed in both the clean and iced configurations of the main rotor for hover and forward flight. Data relative to helicopter performance were gathered as a function of freestream velocity, fuselage angle of incidence, main rotor rpm, rotor collective pitch angle, and radial extent of ice.

The generic ice geometry chosen for this test is representative of a shape that resulted from a 3-min natural icing exposure to a Bell Helicopter model UH-1H helicopter main rotor. The meteorological conditions corresponding to this icing encounter consisted of a free air temperature of −19°C and a liquid water content of 0.7 g/m^3 The ice shape tracing was made at the 46% radial location of the UH-1H main rotor, which ultilizes a 21-in. chord NACA 0012 airfoil. The test program in which the ice shape was observed has been documented by The Ohio State University Aeronautical and Astronautical Research Laboratory (OSU/AARL).[6] Figures 1

Presented as Paper 84-0184 at the AIAA 22nd Aerospace Sciences Meeting, Reno, Nev., Jan. 9-12, 1984; received Feb. 28, 1984.

*Associate Professor, Aerospace Engineering Department. Associate Fellow AIAA.
†Professor and Head, Aerospace Engineering Department. Associate Fellow AIAA.
‡Graduate Research Assistant. Student Member AIAA.

and 2 show a projection of the ice shape as formed in these flight tests compared to the generic ice shapes used in the TAMU wind tunnel test Natural ice roughness because of its relative importance to the aerodynamic characteristics,[7] was simulated on the generic ice shape using an aluminum oxide grit It had been previously noted[8] that an iced surface roughness k/c of 0 001 is typical Therefore, a grit size of 0 028 in was chosen to provide the proper roughness diameter for this test The reader is referred to the work of Korkan et al [4] for details of the fabrication and attachment of the generic ice shape

Model Helicopter Test

The performance degradation of a model helicopter main rotor due to simulated ice accretion has been studied in this test program and makes use of a commercially available radio-controlled model helicopter, as shown in Figs 3 and 4 Ref (5) The model helicopter has a two blade main rotor that incorporates an untwisted NACA 0012 airfoil section with a 2 5 in constant chord and 53 375 in diameter The main rotor is powered by an internal combustion engine of approximately 1/hp Four servomechanisms are installed in the model to control the main rotor rpm, collective pitch, and cyclic pitch (Figs 4 and 5) In this series of tests the collective pitch and rotor rpm were controlled remotely with the cyclic pitch fixed at 0 deg

The model helicopter test was conducted in the TAMU subsonic 7 ft × 10 ft wind tunnel, where the model was mounted on the facility's six component balance The balance is capable of measuring forces about the three principal axes and moments about the main rotor hub The centerline of the model was aligned and fixed with the wind axis Two mountings secured the model one directly beneath the fuselage aligned with the main rotor hub, as shown in Fig 6,

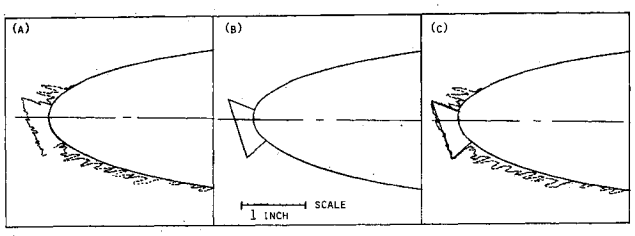

Fig 1 a) Actual ice accretion as documented during flight tests of UH 1H helicopter b) Ice shape used on tunnel model (less roughness) c) Comparison of a) and b)

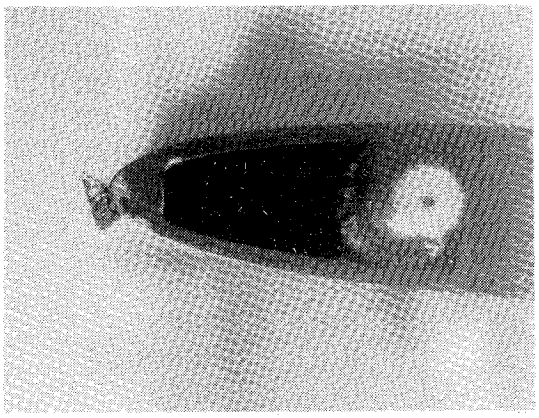

Fig 2 Generic ice shape with roughness attached to leading edge of NACA 0012 airfoil section

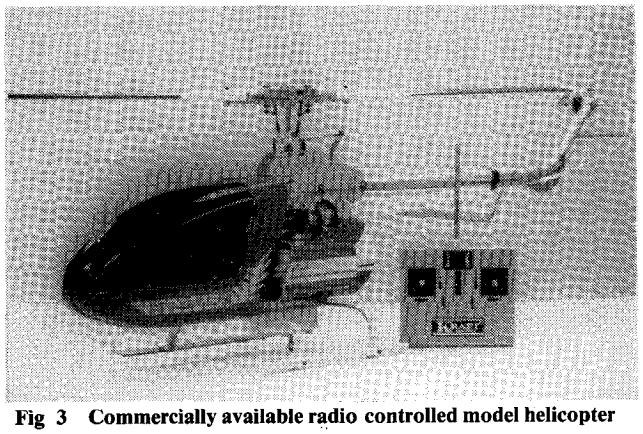

Fig 3 Commercially available radio controlled model helicopter

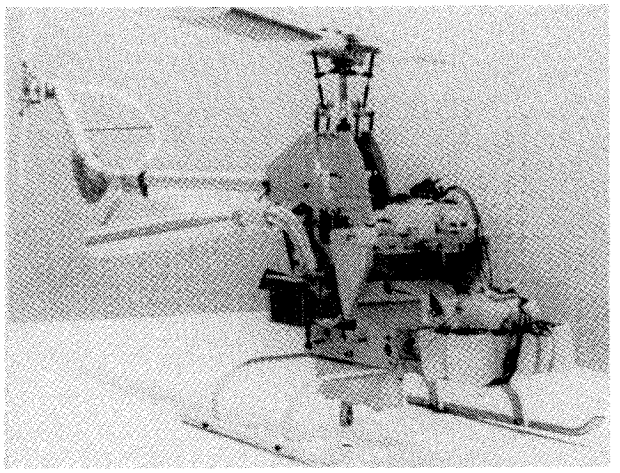

Fig 4 Installation of four servomechanisms in radio controlled model helicopter fuselage

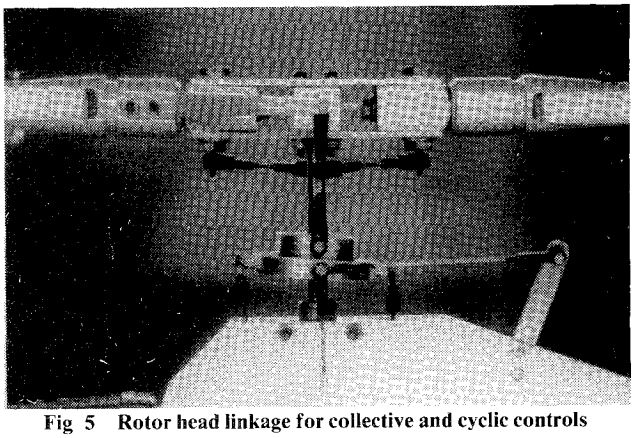

Fig 5 Rotor head linkage for collective and cyclic controls

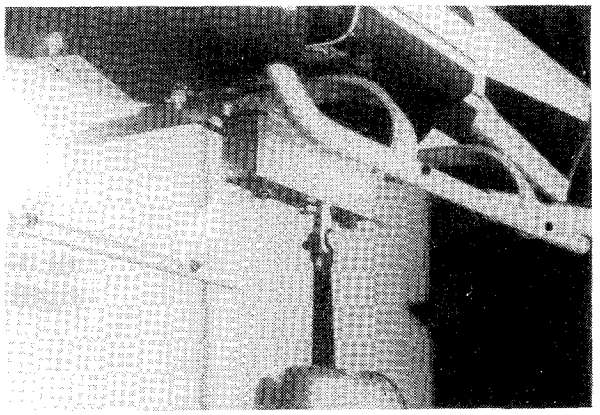

Fig 6 Attachment of model helicopter to wind tunnel strut/six component balance

and the second on the model tail boom. The tail rotor of the helicopter was removed to eliminate the effect on the main rotor torque measurements.

Exhaust from the model helicopter engine initially posed a problem because of exhaust gas accumulation in the closed circuit tunnel. Development and installation of an exhaust removal mechanism that was mounted immediately behind the helicopter greatly reduced this problem (Fig. 7). A splitter plate was attached to the vertical segment of the pipe downstream of the tunnel flow to minimize separation drag on the pipe and reduce interference in the flowfield around the model.

Test Equipment/Data Acquisition

The test utilized the TAMU wind tunnel six-component balance and computer data acquisition system to collect and reduce force and moment data. Model angle of attack, main rotor rpm, main rotor collective pitch, and freestream velocity were also varied and measured.

The helicopter angle of attack was measured using the tail boom of the model, which was horizontal at 0-deg angle of attack and parallel to the rotor disk plane. Positive angle of attack was defined for the helicopter model nose-up.

Main rotor rpm was controlled remotely from the model using the transmitter. In order to accurately determine rotor rpm, a light source above the model was directed toward a photoelectric cell located beneath the helicopter in the wind tunnel floor. An electronic counter connected to the photoelectric cell recorded the interruptions in the light source caused by the rotating rotor blades. The counter was calibrated to provide a digital readout of the main rotor rpm and was determined to be accurate to ± 33 rpm at 1600 rpm.

Collective pitch of the main rotor was also remotely controlled using the transmitter. The collective pitch control was uncoupled from the throttle control so that both collective pitch and RPM could be varied independently to study the effects of each on the main rotor aerodynamics. Collective pitch settings of the rotor blades were determined using a digital voltmeter attached to the radio transmitter. A mechanical pitch indicator was initially placed on the blades to calibrate the pitch setting and provide a correspondence between collective pitch setting and voltmeter reading. With this system, collective pitch could be read to an accuracy of ± 0.1 deg.

The generic ice shape used in this test was geometrically scaled from the simulated ice shape utilized during the NACA 0012 airfoil test[4] and fabricated from balsa wood. It was attached at the same chordwise location as the airfoil simulated ice accretion using a series of templates (see Fig. 1). Again, grit simulating natural ice roughness was applied with the proper scale to provide a roughness of $k/c = 0.0013$.

Test Matrix and Procedure

The model helicopter test consisted of three phases, with the identical test submatrix repeated for each phase. Tare measurements were initially taken of the model with the rotor blades removed, since it was desired to ultimately investigate the performance of the main rotor alone (Fig. 7). Tare measurements were made at velocities of 0 to 40 mph in 10-mph increments. Phase 1 then involved testing the helicopter in the clean or nonicced configuration, obtaining thrust and torque measurements as functions of several variables for both the hover and forward flight condition. In Phase 2, the generic ice shape was applied to the rotor blades to the 85% radial location, and thrust and torque measurements were again made for both hover and forward flight. Simulated ice was finally applied to the 100% radial location of the blades in Phase 3, and, once again, thrust and torque measurements were taken.

After tare measurements were completed, the clean rotor blades were installed on the model and Phase 1 was initiated. Hover data were collected first, with the model helicopter at 0-deg angle of attack and the wind tunnel velocity set at zero. At a collective pitch setting of +1 deg, an rpm sweep was made with data taken at rpm values of 1000 to 1600 rpm in approximately 200-rpm intervals. The collective pitch setting was then changed to +3 deg, and an rpm sweep was performed over the same range of values. A collective pitch setting of +5 deg was then established, and an identical rpm sweep was performed.

The helicopter angle of attack was then changed to -11 deg to represent a forward flight condition (Fig. 8). Wind tunnel velocity was set at 20 mph, and rpm sweeps were made for collective pitch settings of +1, 3, and 5 deg. This procedure was repeated for wind tunnel velocities of 30 and 40 mph. Phase 2 began with the removal of the blades from the model and the addition of generic ice to the leading edge of the main rotor to the 85% radial location. The blades were rebalanced to reduce any dynamic effects and remounted on the model (Fig. 9). The same submatrix followed in Phase 1 was repeated for the helicopter with simulated ice in both the hover and forward flight configuration. The same velocities, collective pitch angles, and rpm values were investigated as were used in phase 1. Phase 3 was identical to phase 2, with the exception of the application of the generic ice shape to the 100% radial location on the main rotor blades. Thrust and

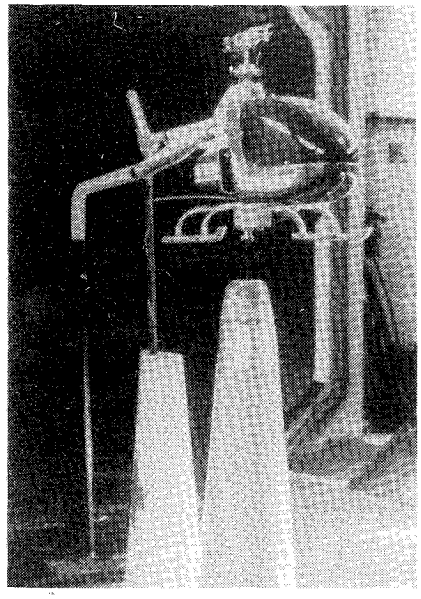

Fig. 7 Model helicopter installed in TAMU 7×10-ft subsonic wind tunnel for tare measurements.

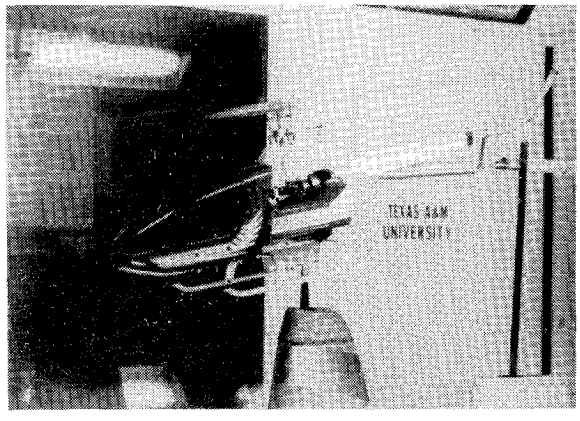

Fig. 8 Model helicopter installed in TAMU 7×10-ft subsonic wind tunnel; forward flight condition ($\alpha = -11$ deg).

torque measurements were again made for the hover and forward flight configurations as functions of freestream velocity, main rotor collective pitch, and rpm.

Care was taken throughout the test to maintain the accuracy of the collective pitch setting and rotor rpm calibrations through periodic checks. Rotor rpm readings were not always taken at exactly 200-rpm intervals, since several of these conditions correspond to points of resonance of the model/balance system. This problem, however, was minimal, never endangering the model or balance to any significant degree. The limits on rotor collective pitch and rpm were set by the mechanical limitations of the model and engine, and the ranges of collective pitch, rpm, and freestream velocity used in the test matrix were chosen to provide a maximum amount of positive lift and propulsive values without jeopardizing the structural integrity of the model.

Helicopter Aerodynamic Coefficients

Main rotor thrust and torque were the primary desired parameters throughout the model helicopter test. Once determined, these and other associated quantities were then reduced to conventional helicopter aerodynamic coefficients for further study.

Thrust coefficient for a helicopter is expressed as

$$C_T = T/\rho A V_{tip}^2 \tag{1}$$

In trim, the thrust of a helicopter is equivalent to the lift force, which acts perpendicular to the rotor disk plane. Therefore, for the forward flight condition, thrust may be resolved into lift and propulsive components. The six-component balance measures forces in the wind-oriented horizontal and vertical directions, such that L_{meas} is equivalent to the lift force and D_{meas} is equivalent to the propulsive force. Rotor thrust may therefore be given by

$$T = (L^2 + D^2)^{1/2}$$

and the thrust coefficient may then be expressed as

$$C_T = (L^2 + D^2)^{1/2}/\rho A V_{tip}^2 \tag{2}$$

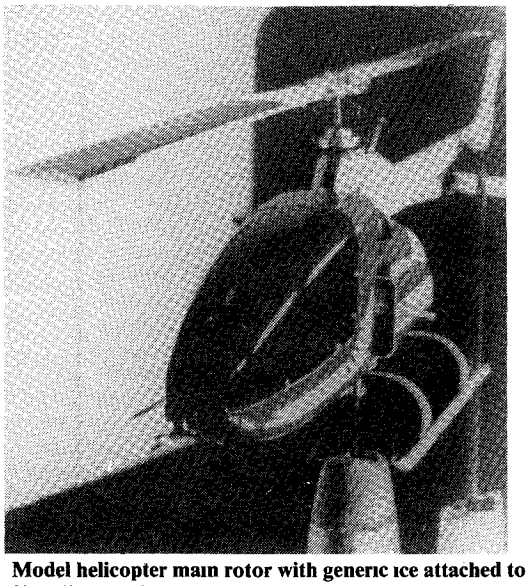

Fig. 9 Model helicopter main rotor with generic ice attached to main rotor 85% radial location.

Torque coefficient for a helicopter is defined by

$$C_Q = Q/(\rho A V_{tip}^2 R_{tip}) \tag{3}$$

For the helicopter it may be noted that since the power coefficient is given by

$$C_P = P/(\rho A V_{tip}^3) \tag{4}$$

and since the rotor shaft power and torque are related by $P = \Omega Q$, C_P is equivalent to C_Q.

To determine the rotor torque values for use in Eq. (3), it may be noted that $Q = Q_{vert}/\cos\alpha$, where Q_{vert} is the vertical component of torque as measured by the balance. If the model helicopter is in the hover mode, $\alpha = 0$ deg and Q is equal to Q_{vert}.

Other variables related to helicopter geometry and motion were also calculated. For example, rotor solidity is given by

$$\sigma = Bc/\Pi R_{tip} \tag{5}$$

and has a constant value of 0.0596 for the model helicopter main rotor. Rotor advance ratio, or tip ratio, is exprssed as

$$\mu = V/V_{tip} = V_\infty \cos\alpha/V_{tip} \tag{6}$$

Freestream and rotor tip Reynolds number values were computed using the expressions

$$Re_\infty = \rho V_\infty c/\mu_\infty \tag{7}$$

$$Re_{tip} = \rho V_{tip} c/\mu_\infty$$

resulting in a tip Reynolds number of 0.5×10^6 to 0.7×10^6

Results

Thrust and torque measurements have been made for the model helicopter in the iced and noniced configurations for both hover ($\alpha = 0$ deg) and forward flight ($\alpha = -11$ deg) conditions. Figure 10 shows the effects of the spanwise simulated ice accretion in hover for a collective pitch setting of +5 deg. An increase of approximately 150% in torque coefficient is noted for a given thrust coefficient when simulated ice is applied to the main rotor 85% radial location. An additional increase of nearly 150% in torque coefficient may be seen when the generic ice is applied out to the rotor 100% radial station. Using the results of Fig. 10, the large increase in torque coefficient that occurs when the outer 15% of the rotor is iced can be shown as in Fig. 11 for a constant C_T and illustrates the performance sensitivity of the rotor tip region to ice accretion. Earlier theoretical studies[2,3,9] have generated similar curves. The apparent exponential decay in thrust coefficient in the rotor tip region for a given torque coefficient, seen in Fig. 12, again illustrates the sensitivity of the outer radii of the main rotor to the ice accretion process.

A similar decline in thrust coefficient for a given torque coefficient as a function of radial location is again shown in Fig. 13, which compares the hover and forward flight configurations. Of note here is the degradation in thrust coefficient, and therefore sensitivity of the rotor tip region, which can be seen to be greater for the forward flight configuration than for hover. The torque coefficient is found to vary similarly in both hover and forward flight as a function of icing radial extent for a constant thrust coefficient (Fig. 14),

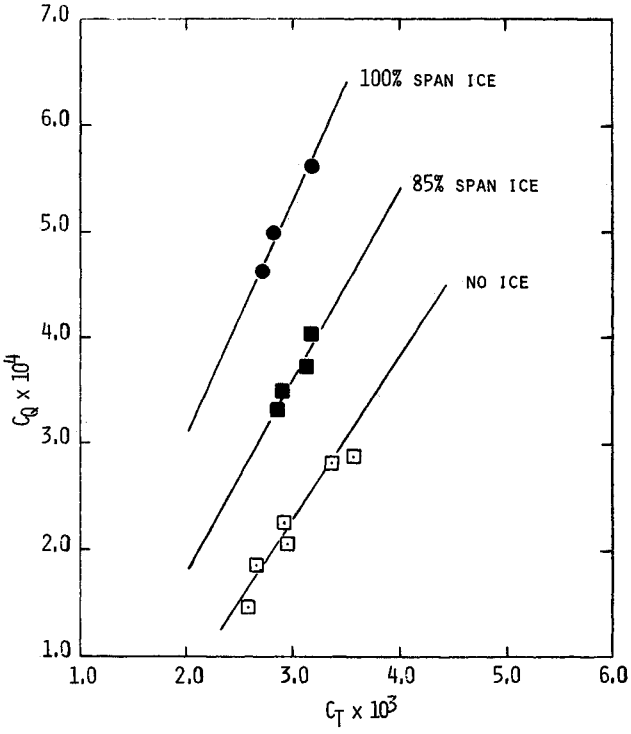

Fig. 10 Variation of torque coefficient vs thrust coefficient for various spanwise additions of generic ice; hover condition ($\theta = 5$ deg).

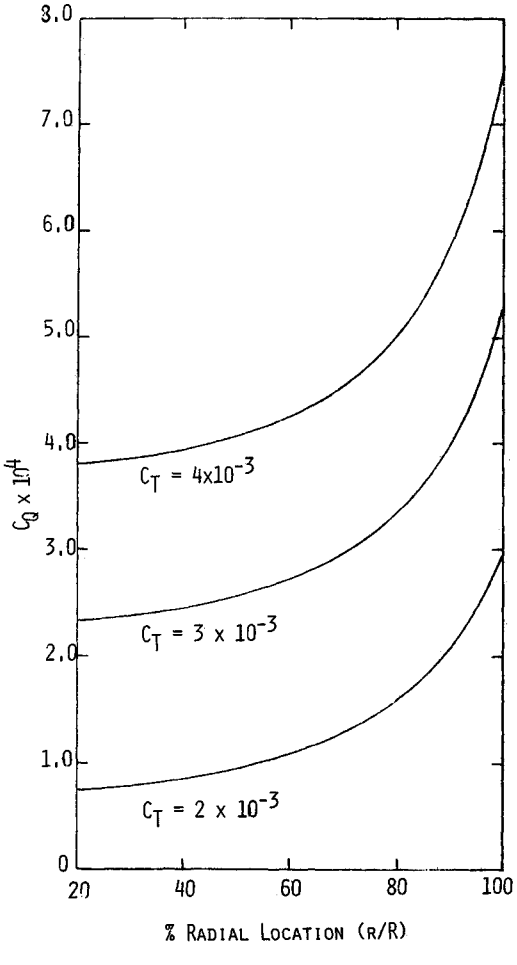

Fig. 11 Increase in torque coefficient as a function of spanwise extent of ice accretion for fixed thrust coefficient; hover condition ($\theta = 5$ deg).

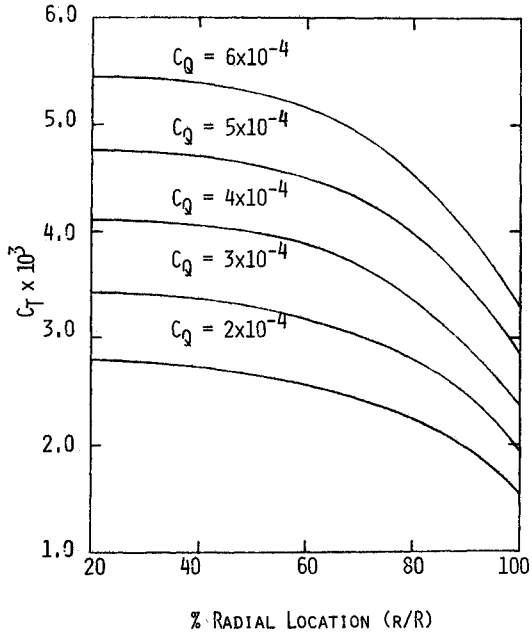

Fig. 12 Decrease in thrust coefficient as a function of spanwise extent of ice accretion for fixed torque coefficient; hover condition ($\theta = 5$ deg).

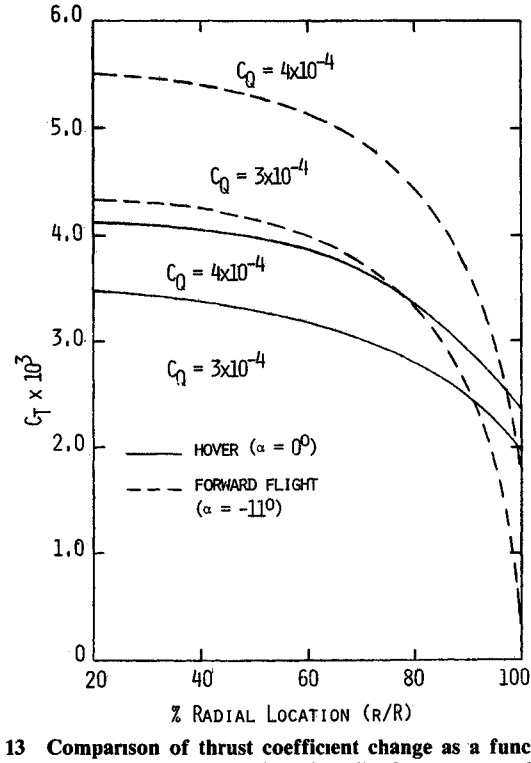

Fig. 13 Comparison of thrust coefficient change as a function of spanwise extent of ice accretion for fixed torque coefficient; hover/forward flight ($\theta = 5$ deg).

with consistently higher torque coefficient values required for the forward flight condition to overcome the additional drag induced by the forward component of velocity.

The forward flight results also show considerable performance degradation due to the simulated ice accretion. Figure 15 illustrates the increase in torque coefficient due to the spanwise ice addition for a given thrust coefficient at a collective pitch angle of +5 deg. An increase of approximately 50% in torque coefficient is found going from the clean to the 85% simulated ice configuration; and a jump

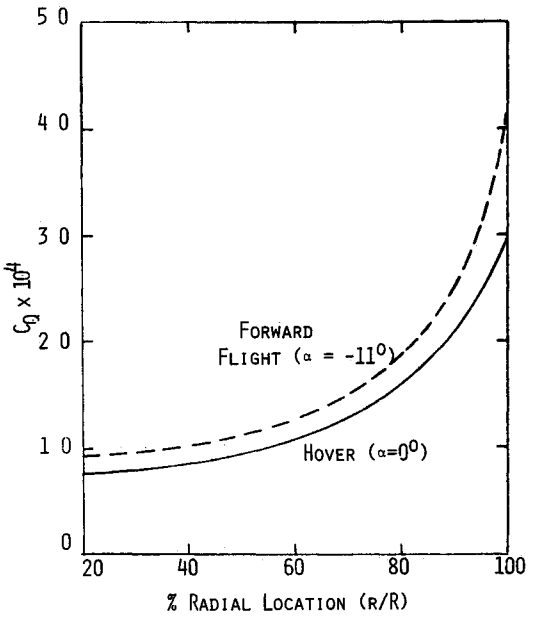

Fig 14 Comparison of torque coefficient change as a function of spanwise extent of ice accretion for a C_T of 2×10^{-3}; hover/forward flight ($\theta=5$ deg)

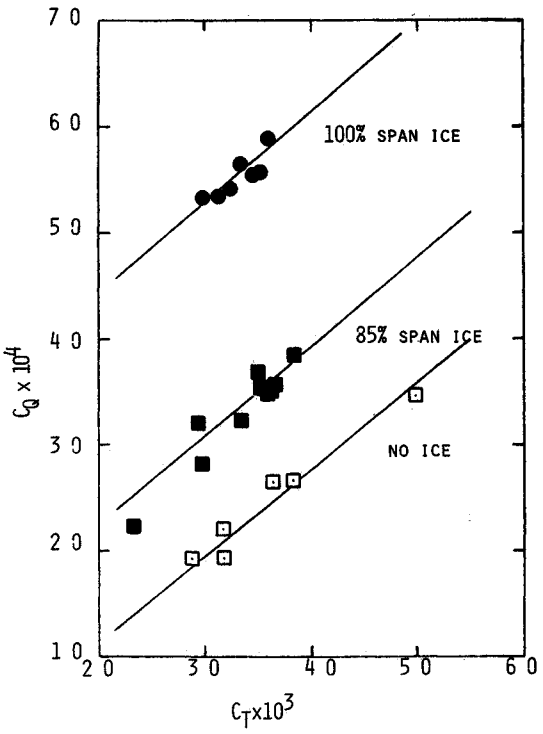

Fig 15 Variation of torque coefficient vs thrust coefficient for various spanwise additions of generic ice; forward flight condition ($\alpha=-11$ deg, $\theta=5$ deg)

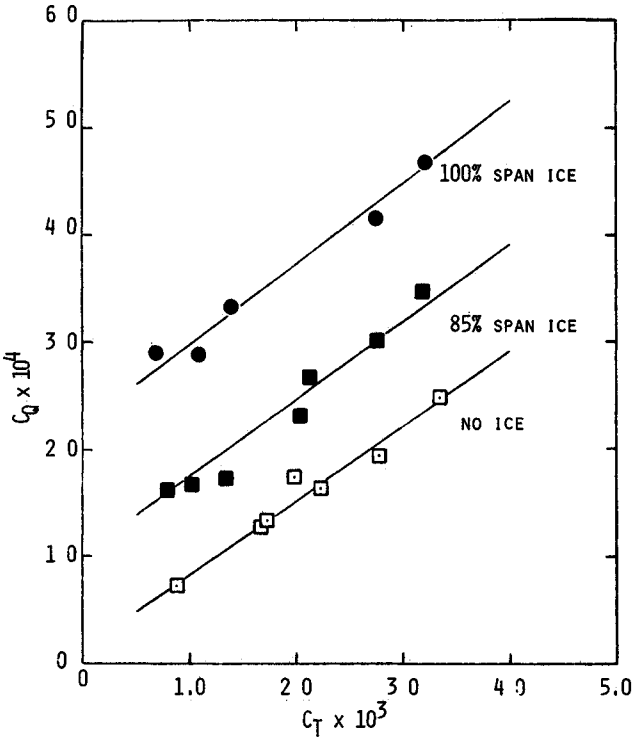

Fig 16 Variation of torque coefficient vs thrust coefficient for various spanwise additions of generic ice; forward flight condition ($\alpha=-11$ deg, $\theta=3$ deg)

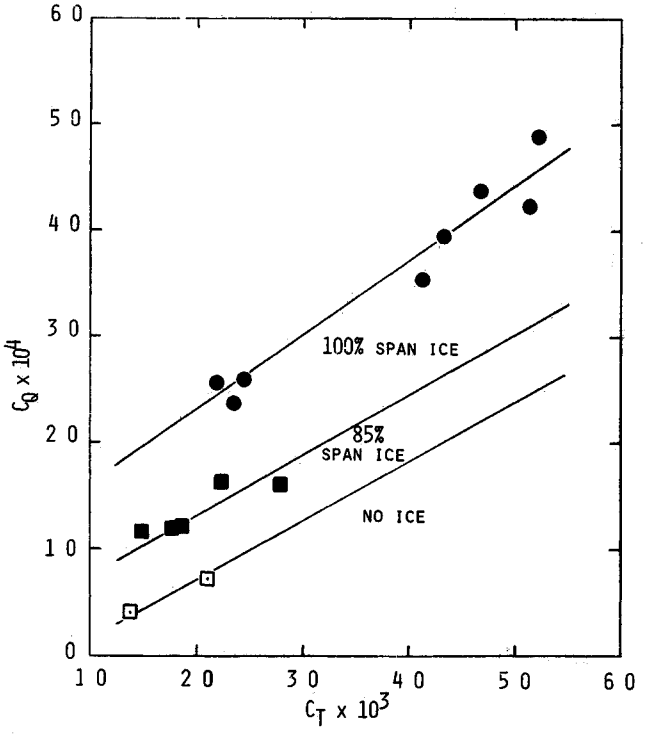

Fig 17 Variation of torque coefficient vs thrust coefficient for various spanwise additions of generic ice; forward flight condition ($\alpha=-11$ deg, $\theta=1$ deg)

of approximately 175% occurs in torque coefficient for the 100% iced condition over the clean configuration at a given thrust coefficient This can be attributed to the extent of leading edge separation and premature boundary layer transition that is induced by the generic ice shape at the higher collective pitch angles Figures 16 and 17 indicate that these phenomena are consistent throughout the data but are more pronounced at the 5-deg collective pitch setting

For a given thrust coefficient, torque coefficient values are plotted as a function of spanwise icing extent as derived from the experimental data in Fig 18 for a collective pitch of +5 deg Here again, as in the hover case, the increase in required torque coefficient is displayed The sensitivity of the rotor tip region is emphasized, e g , for a given thrust coefficient of 3×10^{-3}, the required torque coefficient increases 150% when generic ice is applied to the 100% radial location The sensitivity of the tip region appears to decrease as the thrust coefficient is increased However, even at the highest thrust

coefficient shown, an increase in torque coefficient of 100% results from the application of the ice shape to the 100% rotor radial location Figures 19 and 20 show these same results from collective pitch angles of + 1 and 3 deg

When a constant torque coefficient is maintained and thrust coefficient is plotted as a function of spanwise icing extent, Fig 21 is obtained for a collective pitch of + 5 deg The thrust coefficient is seen to decrease substantially as the generic ice is applied to the rotor 100% radial location Once again, the severe performance degradation associated with icing to the rotor tip is emphasized As in the previous figure, tip sensitivity appears to decrease in terms of percentages with increasing torque coefficient, but considerable thrust degradation still exists for all torque coefficient values investigated Similar results were obtained for pitch angles of +1 and 3 deg, with the decrease in thrust coefficient for a

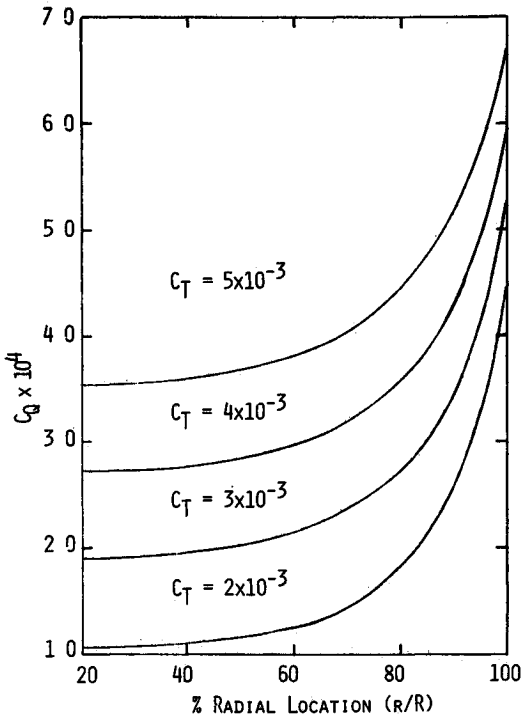

Fig 18 Increase in torque coefficient as a function of spanwise extent of ice accretion for fixed thrust coefficient; forward flight condition ($\alpha = -11$ deg, $\theta = 5$ deg)

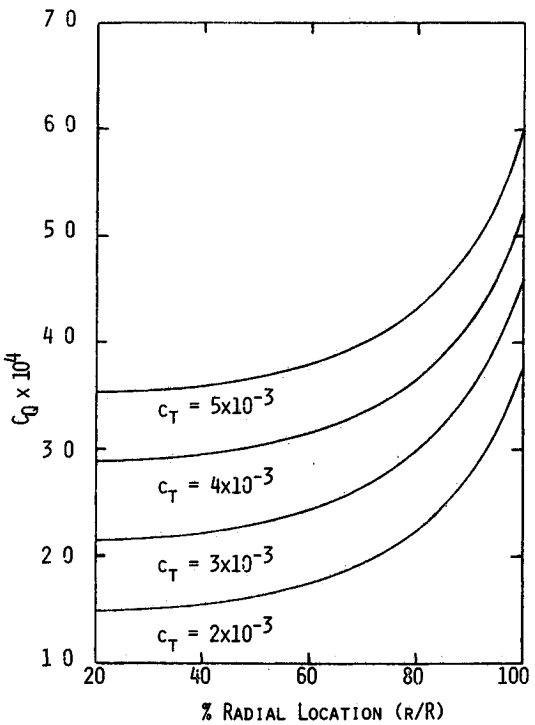

Fig 19 Increase in torque coefficient as a function of spanwise extent of ice accretion for fixed thrust coefficient; forward flight condition ($\alpha = -11$ deg, $\theta = 3$ deg).

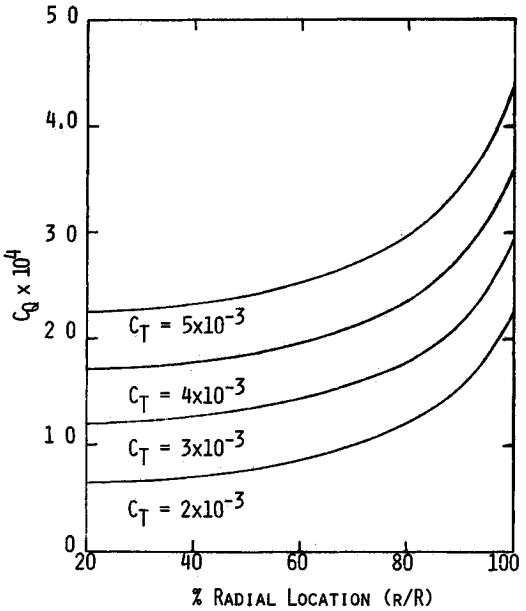

Fig 20 Increase in torque coefficient as a function of spanwise extent of ice accretion for fixed thrust coefficient; forward flight condition ($\alpha = -11$ deg, $\theta = 1$ deg)

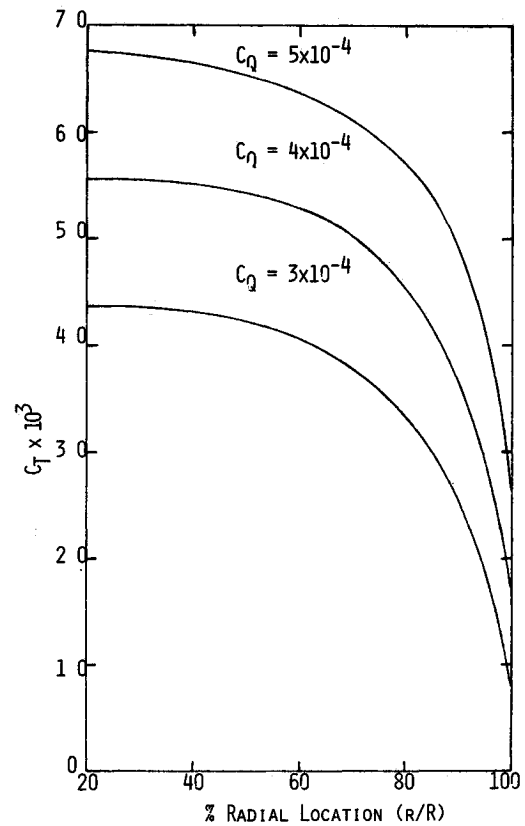

Fig 21 Decrease in thrust coefficient as a function of spanwise extent of ice accretion for fixed torque coefficient; forward flight condition ($\alpha = -11$ deg, $\theta = 5$ deg)

given torque coefficient becoming less severe with decreasing rotor collective pitch angle

Summary

A model helicopter has been used to collect test data and provide an experimental means of studying helicopter performance in the 7×10 ft subsonic wind tunnel at Texas A&M University The present study has demonstrated that use of the model helicopter is a viable means of procuring such test data A simulated generic ice shape was attached to the rotor blades first to the 85% rotor radial location and subsequently to the 100% radial location and performance data were obtained for both hover and forward flight These data illustrate significant degradation in helicopter performance with respect to torque and thrust coefficient when the simulated ice was applied to the rotor blades The sensitivity of the rotor tip region was also demonstrated by noting the considerable additional degradation that occurred when generic ice was applied to the rotor to the 100% radial location as compared with the 85% simulated ice performance values

Various areas of improvement were identified for future consideration Increasing the main rotor chord to 4 in would increase the rotor tip Reynolds number to approximately 1×10^6 A larger chord would also allow more accurate fabrication of the blades and the associated generic ice shapes A larger engine of 2 hp would enable a wider range of torque coefficient values to be investigated Finally, further expansion of the experimental icing data base is desirable for a complete comparison with predicted theoretical value using an existing helicopter performance code [10]

Acknowledgments

This work was supported in part by NASA Lewis Research Center Grant NAG 3 242, "Propeller/Rotor Icing Study" The authors would like to thank Dr R J. Shaw of NASA Lewis Research Center for his continued support and guidance, and the Texas A&M University Subsonic Wind Tunnel group for their participation and assistance in the tests documented in this paper

References

[1]Korkan K D Dadone L and Shaw R J, Performance Degradation of Propeller Systems Due to Rime Ice Accretion *Journal of Aircraft* Vol 21 Jan 1984 pp 44 49

[2]Korkan K. D Dadone, L, and Shaw R J Helicopter Rotor Performance Degradation in Natural Icing Encounter *Journal of Aircraft* Vol 21 Jan 1984 pp 84 85

[3]Korkan K D, Shaw R J and Dadone L Performance Degradation of Helicopter Rotor Systems in Forward Flight Due to Rime Ice Accretion AIAA Paper 83 0029 Jan 1983

[4]Korkan, K D Cross, E J, and Cornell C C. Experimental Study of Performance Degradation of a Model Helicopter Main Rotor with Simulated Ice Shapes AIAA Paper 84 0184 Jan 1984

[5]Korkan K D Cross, E J and Miller T L, Performance Degradation of a Model Helicopter Main Rotor in Hover and For ward Flight with a Generic Ice Shape AIAA Paper 84 0609 March 1984

[6]Lee, J D Documentation of Ice Shapes on the Main Rotor of a UH 1H Helicopter in Hover Aeronautical and Astronautical Research Laboratory, The Ohio State University Columbus Ohio 1984 (to be published), Vol 21 Jan 1984 pp 84 85

[7]Brumby R. E "Wing Surface Roughness, Cause and Effect *DC Flight Approach* Jan 1979 pp 2 7

[8]Bragg, M B and Gregorek G M Aerodynamic Charac teristics of Airfoil with Ice Accretions AIAA Paper 82 0282 Jan 1982

[9]Korkan K D Narramore J C, Dadone L and Shaw R L Performance Evaluation of the XV 15 Tilt Rotor Aircraft in a Natural Icing Encounter AIAA Paper 83 2534 Oct 1983

[10]Hennis R P and McCormick B W A Computer Model for Determining Weapons Release Parameters for a Helicopter in Non Accelerated Flight' Naval Surface Weapons Center/Dahlgren Laboratory Dahlgren Virginia Rept TR 3823 Oct 1978